Hydrogen metabolic patterns driven by Clostridium-Streptococcus community shifts in a continuous stirred tank reactor

R. Palomo-Briones, Eric Trably, N. E. López-Lozano, L. B. Celis, H. O. Méndez-Acosta, Nicolas Bernet, E. Razo-Flores

Hydrogen metabolic patterns driven by *Clostridium-Streptococcus* community shifts in a continuous stirred tank reactor

Rodolfo Palomo-Briones[1], Eric Trably[2], Nguyen Esmeralda López-Lozano[1], Lourdes B. Celis[1], Hugo Oscar Méndez-Acosta[3], Nicolas Bernet[2], Elías Razo-Flores[1]*

[1]División de Ciencias Ambientales, Instituto Potosino de Investigación Científica y Tecnológica. Camino a la Presa San José 2055, Lomas 4a Sección, C.P. 78216, San Luis Potosí, S.L.P., México.

[2]LBE, INRA, Univ Montpellier, 102 avenue des Etangs, 11100 Narbonne, France.

[3]Departamento de Ingeniería Química, CUCEI-Universidad de Guadalajara, Blvd. M. García Barragán 1451, C.P. 44430, Guadalajara, Jal., México

*Corresponding author: erazo@ipicyt.edu.mx, +51 (444) 8342026

ORCID IDs:

Rodolfo Palomo-Briones: 0000-0002-7164-0756

Nicolas Bernet: 0000-0003-2710-3547

Elías Razo-Flores: 0000-0002-8262-695X

ACKNOWLEDGEMENTS

This research was financially supported by the Fondo de Sustentabilidad Energética SENER-CONACYT, Clúster Biocombustibles Gaseosos (project 247006). Rodolfo Palomo-Briones is thankful for the PhD scholarship provided by CONACYT. The authors acknowledge the technical help of Gaëlle Santa-Catalina, Dulce Partida Gutiérrez, Guillermo Vidriales Escobar, and Juan Pablo Rodas Ortiz. The infrastructure provided by CONACYT INFR-2014-01-224220 is also acknowledged.

ABSTRACT

The hydrogen production efficiency in dark fermentation systems is strongly dependent on the occurrence of metabolic pathways derived from the selection of microbial species that either consume molecular hydrogen or outcompete hydrogenogenic bacteria for the organic substrate. In this study, the effect of organic loading rate (OLR) on the hydrogen production performance, the metabolic pathways and the microbial community composition in a continuous system was evaluated. Two bacterial populations, *Clostridium* and *Streptococcus*, were dominant in the microbial community depending on the OLR applied. At low OLR (14.7 - 44.1 $g_{Lactose}$/L-d), *Clostridium sp.* was dominant and directed the system towards the acetate-butyrate fermentation pathway, with a maximum H_2 yield of 2.14 mol_{H2}/mol_{Hexose} obtained at 29.4 $g_{Lactose}$/L-d. Under such conditions, the volumetric hydrogen production rate (VHPR) was between 3.2 - 11.6 L_{H2}/L-d. In contrast, high OLR (58.8 and 88.2 $g_{Lactose}$/L-d) favored the dominance of *Streptococcus sp.* as co-dominant microorganism leading to lactate production. The formate production was also stimulated under these conditions possibly through the Wood-Ljundahl pathway as strategy to dispose the surplus of reduced molecules (e.g. $NADH_2^+$), which theoretically consumed up to 5.72 L_{H2}/L-d. Under such scenario, the H_2 yield was relatively low (0.74 mol_{H2}/mol_{Hexose} at OLR = 58.8 $g_{Lactose}$/L-d) regardless of the higher VHPR reached (13.7 – 14.5 L_{H2}/L-d). Overall, this research brings clear evidence of the intrinsic occurrence of metabolic pathways detrimental for hydrogen production, *i.e.* lactic acid fermentation and formate production, during hydrogen production, suggesting the use of low OLR as strategy to control such undesirable metabolisms.

KEYWORDS

Biohydrogen; Dark fermentation; Lactic Acid Bacteria (LAB); Hydrogen-producing bacteria (HPB): microbial community

1. INTRODUCTION

The development of zero- and low-carbon technologies for energy production is an important milestone in the mitigation of climate change. In this regard, biofuels have gained great attention due to the possibility to revalorize organic wastes generated by industrial, agricultural, and domestic sectors, and minimize the release of additional carbon into the atmosphere.

Biohydrogen (H_2) is an energy carrier that can be distinguished among other fuels due to its high-energy content (120 kJ/g), highly efficient conversion to electric energy, and byproducts-free oxidation. The production of biohydrogen can be performed through four major biological processes: direct and indirect biophotolysis, photofermentation and dark fermentation. Among these, the dark fermentative technology has shown higher production rates and faster and simpler operation than its counterparts. Moreover, dark fermentation is independent of light and the microbial communities have a wide potential to metabolize many types of organic wastes by showing a good performance in spite to fluctuations of environmental conditions through metabolic flexibility (Azwar et al. 2014).

Theoretically, the maximum hydrogen metabolic yield of dark fermentative systems is four moles of H_2 per mole of glucose consumed (Agler et al. 2011). This yield is possible to achieve if only *Clostridium* species are involved in the fermentation by producing acetate as byproduct (Eq. 1).

$$C_6H_{12}O_6 + 2\ H_2O \rightarrow 2\ CH_3COOH + 2\ CO_2 + 4\ H_2 \qquad (1)$$

In practice, H_2 yields are substantially lower than the theoretical value by considering the ideal acetate fermentation (Nath and Das 2004). This is mainly due to the diversity of metabolic routes, i.e., the production of metabolites associated with low or none H_2 production. Such is the case of butyrate, propionate, ethanol, and lactate pathways, among others. Special focus has been paid on the lactate production, which is performed by lactic-acid bacteria (LAB) such as *Lactobacillus*, *Sporolactobacillus*, *Streptococcus,* etc. LAB outcompete hydrogenogenic microorganisms for the carbon source, but are also capable to produce growth-inhibitory compounds (Noike et al. 2002; Sikora et al. 2013; Gomes et al. 2016). Recently, it was reported for continuous stirred tank reactors (CSTR) fed with lactose that LAB co-dominated at large hydraulic retention times (HRT = 18 and 24 h). As consequence, short values of retention time (HRT = 6 and 12

h) were suggested as strategy to control the proliferation of LAB (Palomo-Briones et al. 2017). However, to the best of our knowledge, the effects of the OLR at fixed HRT on LAB in a dark fermentative environment remain unexplored in CSTR systems. This issue is of high interest since the relationship between OLR and LAB can potentially affect the scaling up and economy of the process. On the other hand, H_2 yield can also be shortened due to H_2 consumption through the Wood-Ljungdahl pathway (WLP), which can be carried out by several *Clostridium* species (Diekert and Wohlfarth 1994; Saady 2013). In such pathway, H_2 and CO_2 are combined to produce acetyl-CoA and a diversity of other metabolites (Diekert and Wohlfarth 1994; Tracy et al. 2012; Schuchmann and Müller 2014).

Different authors have reported that LAB and WLP-hydrogenotrophic microorganisms are affected by environmental and operational conditions (e.g. Shanmugam et al. 2014; Carrillo-Reyes et al. 2014; Si et al. 2015). Nevertheless, most studies have been focused on the suppression of either LAB or WLP-hydrogenotrophic microorganisms, although these could be simultaneously present. Under such scenario, the strategies aimed to suppress one of these groups could result in the enrichment of the second one, and *vice versa*. Therefore, this work aims to investigate the effect of OLR on the performance of H_2 production, metabolic pathways and microbial community in a lactose fed CSTR, with special focus on the potential co-occurrence of LAB and WLP-hydrogenotrophic microorganisms.

2. MATERIALS AND METHODS

2.1 Inoculum and substrate

Anaerobic granular sludge from a full-scale UASB reactor treating wastewater from a tequila factory was used as inoculum. Before inoculation, the sludge was disaggregated and heat pretreated at 90-95 °C for 2 hours. The inoculum was added at a final concentration of 4.5 g volatile suspended solids (VSS)/L. Cheese whey powder (CWP) (Darigold, USA) with lactose content of 75.5% was used as substrate at concentrations ranging from 3.7 to 22.5 $g_{lactose}$/L. The feeding solution was supplemented with (mg/L): NH_4Cl, 2100; $MgCl_2 \cdot 6H_2O$, 100; $CuCl_2 \cdot H_2O$, 1.25; $MnCl_2\ 4H_2O$, 7; $FeCl_2\ 4H_2O$, 19.1; $NiCl_2\ 6H_2O$, 102.5. Additionally, phosphate buffer (KH_2PO_4-Na_2HPO_4, pH 5.9) was added to a final concentration of 100 mM.

2.2. Experimental setup

A bioreactor made of glass, with 1 L working volume and 0.3 L of head space (APPLIKON Biotechnologies, USA) was inoculated with the heat pretreated anaerobic sludge. The system was started-up in batch mode for 24 h using CWP at a concentration of 22 $g_{Lactose}$/L. Afterwards, the reactor was shifted to continuous operation at a HRT of 6 h (OLR of 88 $g_{Lactose}$/L-d). In subsequent stages, the OLR was decreased gradually from 88 to 15 $g_{Lactose}$/L-d by modifying the CWP concentration. Stirring, hydraulic retention time, temperature and pH were set and controlled at 250 rpm, 6 h, 37 °C and 5.9, respectively.

2.3 Analytical methods

Liquid samples were collected in a regularly basis and used to determine biomass, chemical oxygen demand (COD), total carbohydrates and volatile fatty acids (VFA). Biomass (as volatile suspended solids, VSS) and soluble COD were quantified as described in the standard methods (APHA/AWWA/WEF 2012). Total carbohydrates were determined by the phenol sulfuric method (Dubois et al. 1956). VFA were quantified from filtered (0.22 mm) samples by capillary electrophoresis (1600A, Agilent Technologies, Waldbronn, Germany) as reported elsewhere (Davila-Vazquez et al. 2008).

The volume of gas produced was measured through a liquid displacement device, and its composition (H_2 and CO_2) was determined through a gas chromatograph equipped with a thermal conductivity detector (6890N, Agilent Technologies, Waldbronn, Germany). All the gas volumes are reported at 1 atm and 273.15 K.

2.4 Capillary Electrophoresis - Single Strand Conformation Polymorphism (CE-SSCP)

The CE-SSCP was performed as described elsewhere (Palomo-Briones et al. 2017). In brief, the bacterial DNA was extracted using the ZR Fungal/Bacterial DNA MiniPrep extraction kit according to manufacturer's instructions (Zymo Research). The amplification of the V3 region of the 16S rRNA genes was performed with Pfu Turbo DNA polymerase (Stratagene, La Jolla, CA, USA) and the universal primers W49 5'-ACGGTCCAGACTCCTACGGG -3' and W104 5'- TTACCGCGGCTGCTGGCAC -3'. The PCR conditions were set as follows (Milferstedt et al. 2013): initial denaturation for 2 min at 94°C; 25 cycles of melting (1 min at 94°C), annealing (1 min at 61°C) and extension (1 min at 72°C); and a final extension step of 10 min at 72°C.

The PCR products were analyzed by CE-SSCP in an ABI 3130 genetic analyzer

(Applied Biosystems, Foster City, CA, USA) as reported by Rochex et al. (2008). The resulting CE-SSCP profiles were aligned with an internal standard (ROX) to consider the inter-sample electrophoretic variability and were normalized with the package *Statfingerprints* available on R platform (R Development Core Team 2011).

The relative abundances of each peak on CE-SSCP profiles were computed with the spectroscopy functionality of OriginPro 8 (first derivative method, both directions, min height 1%, min width 1%). Subsequently, a Pearson's distances matrix was computed using CE-SSCP relative abundances, and it was displayed as a hierarchical cluster dendogram. Such computing was carried out with the *corrplot*, *ggplot* and *ggdendro* packages under R environment (R Development Core Team 2011).

2.5 Illumina sequencing and microbial community analysis

Illumina MiSeq 2x250 paired-end sequencing was performed following the manufacturers protocol (Illumina, USA). The V3-V4 regions of the rRNA gene (~450 bp) were amplified with the primers 341F (5'-CCTACGGGNGGCWGCAG) and 805R (5'-GACTACHVGGGTATCTAATCC) fused with Illumina adapters. The polymerase chain reaction (PCR) was performed using the Phusion High-Fidelity PCR Master Mix with HF Buffer (Thermo Scientific, USA) and the following conditions: initial denaturation step at 95 °C for 3 min, followed by 25 cycles (95 °C, 30 sec; 55 °C, 30 sec; 72 °C, 30 sec) and a final elongation step at 72 °C for 5 min. The PCR products were indexed with Nextera XT index primers in a second PCR (8 cycles) under identical conditions. The resulting amplicons were purified with Agencourt AMPure XP beads (Beckman Coulter, USA) and re-suspended in Illumina buffer. The Illumina sequencing work was carried out by the Unidad Universitaria de Secuenciación Masiva y Bioinformática, Instituto de Biotecnología, UNAM, Cuernavaca, Morelos, México.

The downstream sequence processing was performed using the Quantitative Insights into Microbial Ecology (QIIME) software (Caporaso et al. 2010). The analysis included the merging of the paired sequences with a minimum overlapping of 20 bp and zero errors in the overlapping region. The resulting sequences were quality filtered at a Phred score > Q20. Sequences with less than 350 pb were also eliminated. The chimeric sequences were filtered with the UCHIME 6.1 software (Edgar et al. 2011). Afterwards, open OTU picking at a 97% sequence identity was carried out with the UCLUST algorithm (Edgar 2010) using the SILVA RNA database (128 release) as reference

(https://www.arb-silva.de/download/archive/qiime/). The sequences of this work were deposited in the NCBI BioProject PRJNA392772.

3. RESULTS

3.1 Dark fermentation performance

The CSTR was operated during 80 days under controlled pH (5.9), temperature (37 °C) and HRT (6 h). The reactor was fed at six sequential OLR: 88, 59, 44, 29, 22, and 15 $g_{lactose}$/L-d, referred from now on as Stage I, Stage II, Stage III, Stage IV, Stage V, and Stage VI, respectively. After the first six stages were carried out, an unexpected low performance was noticed in Stage II; thus, the OLR of 59 $g_{lactose}$/L-d was applied again after Stage VI (15 $g_{lactose}$/L-d). In total, the experiments consisted of seven experimental phases as shown in Fig. 1a.

The performance results show that the volumetric hydrogen production rate (VHPR) was directly linked with the OLR (Fig. 1a). A maximal VHPR of 13.9 ± 2.2 L_{H2}/L-d (mean ± SD) was observed in Stage I (OLR of 88.2 $g_{Lactose}$/L-d), while the lowest VHPR of 3.04 ± 0.9 L_{H2}/L-d was found in Stage VI (OLR of 14.7 $g_{Lactose}$/L-d). This confirmed that a successful hydrogenogenic fermentation was established. In terms of H_2 yield, the optimal value of 2.17 ± 0.29 mol_{H2}/mol_{Hexose} (mean ± SD) was found at an OLR of 29.4 $g_{Lactose}$/L-d (Stage IV). Overall, the H_2 yields ranged between 0.67 and 2.17 mol_{H2}/mol_{Hexose} (Fig. 1b).

To determine the main metabolic pathways along the experiment, the VFA were also quantified through capillary electrophoresis. In terms of molar yield, steady state values of acetate and butyrate ranged within 0.13 - 0.53 $mol_{Acetate}/mol_{Hexose}$ and 0.26 - 0.78 $mol_{Butyrate}/mol_{Hexose}$, respectively. On the other hand, the steady state values of formate and lactate were between 0.07 - 0.51 $mol_{Formate}/mol_{Hexose}$ and 0.03 - 0.59 $mol_{Lactate}/mol_{Hexose}$, respectively. Further analysis of the steady states revealed positive correlations between the H_2 yield and the molar yields of acetate and butyrate (Fig. S1, b and d). On the contrary, the molar yields of acetate and butyrate were negatively correlated with the OLR (Fig. S1, f and h). It is worth to mention that during the operation of the CSTR, acetate and butyrate were produced in a roughly constant acetate/butyrate ratio of 0.7, independently of OLR, VHPR and H_2 yield. Moreover, the

H_2 yield was negatively associated with lactate and formate yields (Fig. S1, a and c). The data show that the metabolic routes associated with these two compounds seemed to be favored at relatively high OLR (59 and 88 $g_{Lactose}$/L-d) (Fig. S1, e and g).

Considering that the synthesis of one mole of formate implies the direct or indirect consumption of one mole of H_2, the amount of H_2 depleted in such route was estimated. As result, the maximum amount of H_2 converted to formate was equivalent to 5.7 L_{H2}/L-d at an OLR of 88 $g_{Lactose}$/L-d (Stage I). In contrast, the stage with the minimum production of formate was Stage IV (OLR = 29 g/L-d) during which the equivalent amount of H_2 depleted was of 0.25 ± 0.08 L_{H2}/L-d. Consistently, the maximum H_2 yield was also presented at the same experimental stage (Table 1).

3.2 Microbial community analysis

16S-rRNA amplicons obtained at steady states were analyzed by CE-SSCP to characterize the microbial community structure and reveal the OLR-associated changes. The analysis showed that during the CSTR operation the microbial community was composed principally by three different microorganisms numbered 150, 224 and 910 in reference to the SSCP retention time (Fig. 2b). Based on relative abundances, the microorganism numbered 910 was dominant at OLR ≥ 59 $g_{Lactose}$/L-d. In contrast, two different organisms (150 and 224) dominated at OLR ≤ 44 $g_{Lactose}$/L-d. An Unweighted Pair Group Method with Arithmetic Mean (UPGMA) analysis of the CE-SSCP profiles showed a clear association among stages I, II and VII, regardless of the amount of time separating such experimental stages (Fig. 2a). On the other hand, stages III, IV, V and VI were also clustered with each other. Overall, two cohesive and OLR-dependent microbial community groups were unveiled.

To identify the microbial genera involved in the fermentation, the V3-V4 regions of 16S-rRNA gene were sequenced and compared with the Silva 16S RNA database to assign taxonomy. The 16S RNA sequencing resulted in 664101 ± 67239 high quality reads per sample, grouped in 14559 operational taxonomic units (OTU), identified up to the genus level. Overall, the results showed the presence of two main genera that dominated all along the fermentation time, *Clostridium* and *Streptococcus* (Fig. 3). To identify and characterize the link between CE-SSCP and 16S-rRNA sequencing, a correlation analysis was conducted. The results showed that *Clostridium* was well correlated with microorganisms numbered 150 (R^2=0.96, $p<0.01$) and 224 (R^2=0.96, $p<0.01$) while *Streptococcus* was strongly correlated with the microorganism numbered

910 (R^2=0.98, p<0.01). Therefore, 16S-rRNA sequencing results were utilized for microbial community analysis.

As shown in Fig. 3, *Clostridium* and *Streptococcus* accounted for more than 88% of the relative abundance, while other microbial genera such as *Enterobacter*, *Escherichia*, *Lactobacillus*, *Lactococcus* and *Enterococcus*, remained subdominant. In general, the relative abundance of *Clostridium* was strongly associated with the reduction of the OLR, while the *Streptococcus* abundance was higher as the OLR increased (Fig. 3b).

In order to better understand and visualize the relationship between the microbial community composition and the performance of the reactor (i.e. VHPR, OLR, H_2 yield, and VFA yields), a Principal Components Analysis (PCA) was conducted (Fig. 4). Two principal components accounted for more than 80 percent of the dataset variance. The results showed a clear relationship between *Clostridium* and the butyrate and acetate yields. On the other hand, *Streptococcus* was strongly linked to VHPR, OLR, and lactate yield. Interestingly, formate and H_2 yields showed negative influence on each other, confirming the aforementioned negative correlation between these two metabolic products. Nevertheless, no linear relationship was found between formate and H_2 yields with the *Clostridium* nor *Streptococcus* abundance.

4. DISCUSSION

The continuous H_2 production from CWP was successfully established in a continuous reactor and was comparable to previous works under similar conditions (Davila-Vazquez et al. 2009; Cota-Navarro et al. 2011). Davila-Vazquez et al. (2009) reported a VHPR of 12.5 L_{H2}/L-d at an OLR of 92.4 $g_{Lactose}$/L-d, while Cota-Navarro et al. (2011) reported a VHPR of 16.1 L_{H2}/L-d at an OLR of 95 $g_{Lactose}$/L-d. Both values were quite similar to the VHPR found in this research (13.7 ± 1.3 L_{H2}/L-d at an OLR of 88 $g_{Lactose}$/L-d) and demonstrate the reliability and reproducibility of dark fermentation with CSTR systems.

Next generation sequencing analysis revealed that a low diverse and highly specialized microbial community composed mainly by *Clostridium* and *Streptococcus* drove the lactose-based dark-fermentative hydrogen production in the CSTR. Such a low microbial diversity was previously described as a common characteristic of hydrogen-producing bioreactors (Etchebehere et al. 2016). This feature becomes accentuated due

to the strong selection pressure that is typical of suspended-growth systems. Interestingly, the relative abundances of these genera were negatively associated to each other, suggesting competitive interactions. In addition, the changes in the OLR had a critical impact on the microbial community distribution and subsequent metabolites production, including H_2. In this regard, two different OLR-dependent states of operation were identified.

4.1 Highly efficient H_2 producing phase

The operation of the dark fermentative CSTR under OLR ≤ 44.1 $g_{Lactose}$/L-d was found to favor the efficiency of H_2 production, i.e. the H_2 yield. At such conditions (Stages III-VI), the microbial community was clearly dominated by microorganisms from the *Clostridium* genera (Fig. 3). These microorganisms have been widely found in dark fermentative systems and have been identified as highly desirable species for H_2 production (Cabrol et al. 2017). Theoretically, *Clostridium* species are capable to produce H_2 with a metabolic yield of 4 mol_{H2}/mol_{Hexose} following the acetate pathway (Eq. 1). However, this route is only feasible at low H_2 partial pressures (P_{H2} < 60 Pa); otherwise, the synthesis of H_2 from NADH becomes thermodynamically unfavorable (Angenent et al. 2004). *Clostridium* microorganisms can also perform the synthesis of H_2 though the butyrate pathway ($C_6H_{12}O_6 \rightarrow CH_3\text{-}CH_2\text{-}CH_2\text{-}COOH + 2\ CO_2 + 2H_2$) which leads to a theoretical H_2 yield of 2 mol_{H2}/mol_{Hexose}. These two pathways (acetate and butyrate) are considered as the most efficient pathways for H_2 production through the dark fermentative process.

In agreement, acetate and butyrate were the principal VFA produced under the dominance of *Clostridium* genera (Fig. 2c); the H_2 yield reached a maximum mean value of 2.14 $mol_{H2}/mol_{Hexose\text{-}consumed}$ (Stage IV). Considering the metabolic limitation and that most of literature has reported H_2 yields of about 1.3 mol_{H2}/mol_{Hexose}, the results of the present study at OLR ≤ 44.1 $g_{Lactose}$/L-d are quite remarkable. On the other hand, the VHPR (3.2 - 11.6 L_{H2}/L-d) was still low, compared to that reported in other studies (Davila-Vazquez et al. 2009; Lee et al. 2012; Sivagurunathan and Lin 2016). The increase of the OLR could possibly lead to higher VHPR but, as discussed in the following section, the increase of the organic loading rate could cause new problems that have significant impacts on the efficiency of the process.

4.2 Lactate and formate favored at high OLR

The operation of the CSTR at OLR ≥ 58.8 $g_{Lactose}$/L-d caused an important increase in the VHPR (12.3 - 14.5 L/L-d) while the efficiency of the process was notably reduced (1.21 - 1.9 mol_{H2}/mol_{Hexose}). This seems to be a disjunction point between productivity and efficiency of hydrogen production. A possible explanation for such phenomenon is that, under high OLR conditions, H_2 is produced in such an amount that probably it is not transferred off the system with the required efficiency, i.e. the process is limited by mass transfer. Under such conditions, the microorganisms pursue alternative pathways to dispose the electrons gathered from the organic substrate and tend to produce less H_2 (Nath and Das 2004). The results clearly showed that the alternative metabolic routes were lactate and formate production.

The presence of lactate is a clear signal of the occurrence of lactic acid fermentation, which is usually found in dark fermentative systems (Baghchehsaraee et al. 2010; Sikora et al. 2013; Etchebehere et al. 2016). Such finding was confirmed by the presence of *Streptococcus*, a lactic acid bacterium that was mainly present at relatively high OLR (Fig. 3). *Streptococcus* has been previously found inside hydrogenogenic granules where they presumably strengthen the granule structure (Hung et al. 2011). Davila-Vazquez et al. (2009) also reported the presence of *Streptococcus* in a CSTR fed with lactose-CWP at an OLR of 92.4 and 138.6 $g_{Lactose}$/L-d with HRT of 6 h and 4 h, respectively. In a recent report, it was concluded that the HRT is a factor of selection that strongly affects the microbial community composition; it was shown that LAB (*Streptococcacea* and *Sporolactobacillaceae*) could be eliminated at low HRT (6 h) (Palomo-Briones et al. 2017). In the present work, although the HRT was maintained at 6 h, the elimination of LAB was only possible when using low OLR values.

The microbial community dynamics is often associated to the differences in growth capabilities of the involved species. However, in the case of LAB and *Clostridium*, different studies have reported similar Monod-type growth kinetics (in terms of μ_{max} and K_S) with lactose (Table 2); therefore, the community behavior observed in the present study could be barely explained by kinetic differences. Rather, the community structure could be the result of product inhibitory effects over *Clostridium* at high OLR that allowed LAB to better compete for the substrate uptake. Napoli et al. (2011) reported that *Clostridium acetobutylicum* could be inhibited by the accumulation of acetate and butyrate, with critical concentrations of 26 mmol/L and 34 mmol/L, respectively. In the present study, the acetate and butyrate concentrations were in the range of those

reported as inhibitory by Napoli et al., (2011) and strongly associated with the OLR, reaching their highest concentrations at OLR of 88.2 $g_{Lactose}$/L-d (Table 1). On the contrary, the lowest concentrations of acetate and butyrate were observed at OLR of 15 $g_{Lactose}$/L-d, where *Clostridium* was strongly dominant. Therefore, the inhibition phenomenon seems to be an important driver of the *Clostridium-Streptococcus* dynamics.

Considering the microbial community results, the formate synthesis was probably performed by *Clostridium* species. Theoretically, the production of formate is carried out with the catalysis of the pyruvate:formate lyase (*pfl*) and the formate dehydrogenase (*fdh)*. The former enzyme catalyzes the activation of pyruvate to acetyl-CoA with the concomitant production of formate and CO_2, while the later catalyzes the synthesis of formate from $NADH_2^+$ and CO_2. The *pfl* is broadly found in facultative anaerobes, but it has been also found in the genome of different *Clostridium* species such as *C. butyricum* , *C. acetobutylicum*, *C. beijirinkii*, *C. pasteurianum*, and *C. tyrobutyricum* (Nölling et al. 2001; Pyne et al. 2014; Noar et al. 2014; Kwok et al. 2014; Lee et al. 2016)

In addition, the gene of *fdh* enzyme has been reported to be part of the genome of different *Clostridium* species, such as *C. carboxidivorans* (Bruant et al. 2010), *C. ljungdahlii* (Köpke et al. 2010)*, C. beijirinkii* (Milne et al. 2011)*,* and *C. acetobutylicum* (Senger and Papoutsakis 2008). *fdh* is also the first enzyme to participate in the WLP which leads to the synthesis of acetate (homoacetogenesis). Considering the actual concentrations of VFA, acetate and formate synthesis from H_2 and CO_2 are both favorable reactions (Table 3). Nevertheless, no evidence of autotrophic acetate (homoacetogenesis) was found in the experiments here reported. Therefore, formate was probably the main hydrogen sink under the conditions tested.

To determine the exact mechanism of formate production will require further studies. However, as formate was OLR dependent, our hypothesis is that such conditions caused an excess of reduced equivalents ($NADH_2^+$, Fd_{red}) that accumulated in the cell due to kinetic limitation at the hydrogenases (*hyd*) level. The primary method to dispose electrons is by the action of hydrogenases, but their activity is retro-inhibited at high concentrations of H_2. Thus, the production of formate was a possible strategy to dispose the excess of electrons gathered from the organic substrate, and maintain NAD^+/NADH and Fd_{ox}/Fd_{red} equilibriums. Under this hypothesis, not only homoacetogenesis but also

formic acid synthesis through either the *fdh* (*i.e.* WLP) or *pfl* route plays an important role in H_2 consumption that deserves to be studied with detail.

To overcome the detrimental consequences of formate synthesis and boost hydrogen production, new ways to recover H_2 (and possibly CO_2 as well) as soon as it is produced should be developed and implemented. In this regard, different alternatives have been proposed with the aim to increase H_2 productivities. Nasr et al. (2015) reported 22% increase of H_2 yield using KOH pellets to capture CO_2 *in situ*. The capture of CO_2, as discussed by the authors, favored the shift of the hydrogenogenic reactions to the forward direction (i.e. production of H_2). Moreover, CO_2 sequestration also had an influence on the metabolic pathways, favoring acetate productivity while lowering butyrate production. Other researchers conducted experiments under a continuous release of biogas generated maintaining the headspace pressure at or below of 0.116 atm (Esquivel-Elizondo et al. 2014). They found that under such conditions the system enhanced in terms of H_2 yield (from 1.2 to 1.9 mol H_2 /$mol_{glucose}$) and VHPR (from 36 to 108 mL H_2/L-h) in comparison to their control (gas released when pressure was above 1.36 atm).

5. CONCLUSIONS

This research shows the results of continuous H_2 production in a CSTR from cheese whey powder as substrate. Overall, the microbial community was dominated by three bacterial phylotypes from two main genera, *Clostridium* and *Streptococcus,* whose relative abundances were strongly affected by the OLR. The shift in the microbial community composition also influenced the metabolic pathways performed. At low OLR (14.7-44.1 $g_{Lactose}$/L-d), *Clostridium* was the dominant genus and drove the system to a highly efficient acetate-butyrate fermentation with a maximum H_2 yield of 2.14 $mol_{H2}/mol_{Hex\text{-}consumed}$ obtained at an OLR of 29.4 $g_{Lactose}$/L-d. In contrast, high OLR (58.8 and 88.2 $g_{Lactose}$/L-d) caused an increase of acetate and butyrate concentrations, which possibly inhibited *Clostridium* growth and prompted the competition of LAB. Under such scenario, *Streptococcus* aroused as the co-dominant microorganism and was successfully associated with the production of lactate. In consequence, the efficiency of H_2 production was negatively affected (min H_2 yield=0.74 mol_{H2}/mol_{Hexose} at OLR=58.8 $g_{Lactose}$/L-d) regardless of the higher VHPR observed (max 13.7 L/L-d) in comparison with low OLR conditions. Moreover, it was found that H_2 was probably consumed

through metabolic pathways leading to the production of formate as alternative to dispose the excess of reduced equivalents. Most probably, either the *pfl* or *fdh* (through the WLP) were possible involved in such phenomenon. Thus, not only homoacetogenesis but also formic acid synthesis plays an important role in H_2 consumption has and deserves to be studied with detail. An overall analysis of the results of this research revealed that the detrimental metabolisms of lactic acid fermentation and formate synthesis could be minimized at low OLR. Otherwise, the effective liberation of H_2 right after its production will be also required.

6. CONFLICT OF INTEREST

The authors declare that they have no conflict of interest.

7. ETHICAL STATEMENT

The authors confirm that the article does not contain any studies with human participants or animals.

8. SUPPORTING INFORMATION AVAILABLE

Additional supporting information is available in the online version of this article at the publisher's web-site.

9. REFERENCES

Agler MT, Wrenn B a, Zinder SH, Angenent LT (2011) Waste to bioproduct conversion with undefined mixed cultures: the carboxylate platform. Trends Biotechnol 29:70–78. doi: 10.1016/j.tibtech.2010.11.006

Altiok D, Tokatli F, Harsa S (2006) Kinetic modelling of lactic acid production from whey byLactobacillus casei (NRRL B-441). J Chem Technol Biotechnol 81:1190–1197. doi: 10.1002/jctb.1512

Angenent LT, Karim K, Al-Dahhan MH, Wrenn B a., Domíguez-Espinosa R (2004) Production of bioenergy and biochemicals from industrial and agricultural wastewater. Trends Biotechnol 22:477–485. doi: 10.1016/j.tibtech.2004.07.001

APHA/AWWA/WEF (2012) Standard Methods for the Examination of Water and

Wastewater.

Azwar MY, Hussain M a., Abdul-Wahab AK (2014) Development of biohydrogen production by photobiological, fermentation and electrochemical processes: A review. Renew Sustain Energy Rev 31:158–173. doi: 10.1016/j.rser.2013.11.022

Baghchehsaraee B, Nakhla G, Karamanev D, Margaritis A (2010) Fermentative hydrogen production by diverse microflora. Int J Hydrogen Energy 35:5021–5027. doi: 10.1016/j.ijhydene.2009.08.072

Berry AR, Franco CMM, Zhang W, Middelberg APJ (1999) Growth and lactic acid production in batch culture of Lactobacillus rhamnosus in a defined medium. Biotechnol Lett 21:163–167. doi: 10.1023/A:1005483609065

Boonmee M, Leksawasdi N, Bridge W, Rogers PL (2003) Batch and continuous culture of Lactococcus lactis NZ133: Experimental data and model development. Biochem Eng J 14:127–135. doi: 10.1016/S1369-703X(02)00171-7

Bruant G, Lévesque MJ, Peter C, Guiot SR, Masson L (2010) Genomic analysis of carbon monoxide utilization and butanol production by clostridium carboxidivorans strain P7T. PLoS One 5:1–12. doi: 10.1371/journal.pone.0013033

Burgos-Rubio CN, Okos MR, Wankat PC (2000) Kinetic study of the conversion of different substrates to lactic acid using Lactobacillus bulgaricus. Biotechnol Prog 16:305–314. doi: 10.1021/bp000022p

Cabrol L, Marone A, Tapia-Venegas E, Steyer J-P, Ruiz-Filippi G, Trably E (2017) Microbial ecology of fermentative hydrogen producing bioprocesses: useful insights for driving the ecosystem function. FEMS Microbiol Rev 41:158–181. doi: 10.1093/femsre/fuw043

Caporaso JG, Kuczynski J, Stombaugh J, Bittinger K, Bushman FD, Costello EK, Fierer N, Peña AG, Goodrich JK, Gordon JI, Huttley GA, Kelley ST, Knights D, Koenig JE, Ley RE, Lozupone CA, McDonald D, Muegge BD, Pirrung M, Reeder J, Sevinsky JR, Turnbaugh PJ, Walters WA, Widmann J, Yatsunenko T, Zaneveld J, Knight R (2010) QIIME allows analysis of high-throughput community sequencing data. Nat Methods 7:335–336. doi: 10.1038/nmeth.f.303

Carrillo-Reyes J, Celis LB, Alatriste-Mondragón F, Razo-Flores E (2014) Decreasing methane production in hydrogenogenic UASB reactors fed with cheese whey. Biomass and Bioenergy 63:101–108. doi: 10.1016/j.biombioe.2014.01.050

Cota-Navarro CB, Carrillo-Reyes J, Davila-Vazquez G, Alatriste-Mondragón F, Razo-Flores E (2011) Continuous hydrogen and methane production in a two-stage

cheese whey fermentation system. Water Sci Technol 64:367–374. doi: 10.2166/wst.2011.631

Davila-Vazquez G, Alatriste-Mondragón F, de León-Rodríguez A, Razo-Flores E (2008) Fermentative hydrogen production in batch experiments using lactose, cheese whey and glucose: Influence of initial substrate concentration and pH. Int J Hydrogen Energy 33:4989–4997. doi: 10.1016/j.ijhydene.2008.06.065

Davila-Vazquez G, Cota-Navarro CB, Rosales-Colunga LM, de León-Rodríguez A, Razo-Flores E (2009) Continuous biohydrogen production using cheese whey: Improving the hydrogen production rate. Int J Hydrogen Energy 34:4296–4304. doi: 10.1016/j.ijhydene.2009.02.063

Diekert G, Wohlfarth G (1994) Metabolism of homocetogens. Antonie Van Leeuwenhoek 66:209–21.

Dubois M, GILLES KA, HAMILTON JK, REBERS PA, SMITH F (1956) Colorimetric Method for Determination of Sugars and Related Substances. Anal Chem 28:350–356.

Edgar RC (2010) Search and clustering orders of magnitude faster than BLAST. Bioinformatics 26:2460–2461. doi: 10.1093/bioinformatics/btq461

Edgar RC, Haas BJ, Clemente JC, Quince C, Knight R (2011) UCHIME improves sensitivity and speed of chimera detection. Bioinformatics 27:2194–2200. doi: 10.1093/bioinformatics/btr381

Esquivel-Elizondo S, Chairez I, Salgado E, Aranda JS, Baquerizo G, Garcia-Pe??a EI (2014) Controlled continuous bio-hydrogen production using different biogas release strategies. Appl Biochem Biotechnol 173:1737–1751. doi: 10.1007/s12010-014-0961-8

Etchebehere C, Castelló E, Wenzel J, del Pilar Anzola-Rojas M, Borzacconi L, Buitrón G, Cabrol L, Carminato VM, Carrillo-Reyes J, Cisneros-Pérez C, Fuentes L, Moreno-Andrade I, Razo-Flores E, Filippi GR, Tapia-Venegas E, Toledo-Alarcón J, Zaiat M (2016) Microbial communities from 20 different hydrogen-producing reactors studied by 454 pyrosequencing. Appl Microbiol Biotechnol 100:3371–3384. doi: 10.1007/s00253-016-7325-y

Gomes SD, Fuess LT, Mañunga T, Feitosa de Lima Gomes PC, Zaiat M (2016) Bacteriocins of lactic acid bacteria as a hindering factor for biohydrogen production from cassava flour wastewater in a continuous multiple tube reactor. Int J Hydrogen Energy 41:8120–8131. doi: 10.1016/j.ijhydene.2015.11.186

Hung C-H, Cheng C-H, Guan D-W, Wang S-T, Hsu S-C, Liang C-M (2011) Interactions between Clostridium sp. and other facultative anaerobes in a self-formed granular sludge hydrogen-producing bioreactor. Int J Hydrogen Energy 36:8704–8711. doi: 10.1016/j.ijhydene.2010.06.010

Kleerebezem R, Van Loosdrecht MCM (2010) A Generalized Method for Thermodynamic State Analysis of Environmental Systems. Crit Rev Environ Sci Technol 40:1–54. doi: 10.1080/10643380802000974

Köpke M, Held C, Hujer S, Liesegang H, Wiezer A, Wollherr A, Ehrenreich A, Liebl W, Gottschalk G, Dürre P (2010) Clostridium ljungdahlii represents a microbial production platform based on syngas. Proc Natl Acad Sci 107:13087–13092. doi: 10.1073/pnas.1004716107

Kwok JSL, Ip M, Chan T-F, Lam W-Y, Tsui SKW (2014) Draft Genome Sequence of Clostridium butyricum Strain NOR 33234, Isolated from an Elderly Patient with Diarrhea. Genome Announc. doi: 10.1128/genomeA.01356-14

Lee J, Jang YS, Han MJ, Kim JY, Lee SY (2016) Deciphering Clostridium tyrobutyricum metabolism based on the whole-genome sequence and proteome analyses. MBio 7:1–12. doi: 10.1128/mBio.00743-16

Lee K-S, Tseng T-S, Liu Y-W, Hsiao Y-D (2012) Enhancing the performance of dark fermentative hydrogen production using a reduced pressure fermentation strategy. Int J Hydrogen Energy 37:15556–15562. doi: 10.1016/j.ijhydene.2012.04.039

Milferstedt K, Santa-Catalina G, Godon J-J, Escudié R, Bernet N (2013) Disturbance Frequency Determines Morphology and Community Development in Multi-Species Biofilm at the Landscape Scale. PLoS One 8:e80692. doi: 10.1371/journal.pone.0080692

Milne CB, Eddy J a, Raju R, Ardekani S, Kim P-J, Senger RS, Jin Y-S, Blaschek HP, Price ND (2011) Metabolic network reconstruction and genome-scale model of butanol-producing strain Clostridium beijerinckii NCIMB 8052. BMC Syst Biol 5:130. doi: 10.1186/1752-0509-5-130

Napoli F, Olivieri G, Russo ME, Marzocchella Antonio A, Salatino P (2011) Continuous lactose fermentation by Clostridium acetobutylicum - Assessment of acidogenesis kinetics. Bioresour Technol 102:1608–1614. doi: 10.1016/j.biortech.2010.09.004

Nasr N, Velayutham P, Elbeshbishy E, Nakhla G, El Naggar MH, Khafipour E, Derakhshani H, Levin DB, Hafez H (2015) Effect of headspace carbon dioxide sequestration on microbial biohydrogen communities. Int J Hydrogen Energy

40:9966–9976. doi: 10.1016/j.ijhydene.2015.06.077

Nath K, Das D (2004) Improvement of fermentative hydrogen production: Various approaches. Appl Microbiol Biotechnol 65:520–529. doi: 10.1007/s00253-004-1644-0

Noar J, Makwana ST, Bruno-Bárcena JM (2014) Complete Genome Sequence of Solvent-Tolerant Clostridium beijerinckii Strain SA-1. Genome Announc. doi: 10.1128/genomeA.01310-14

Noike T, Takabatakea H, Mizunoc O, Ohbab M (2002) Inhibition of hydrogen fermentation of organic wastes by lactic acid bacteria. Int J Hydrogen Energy 27:1367–1371. doi: 10.1016/S0360-3199(02)00120-9

Nölling J, Breton G, Omelchenko M V, Kira S, Zeng Q, Gibson R, Lee HM, Dubois J, Qiu D, Hitti J, Sequencing GTC, Wolf YI, Tatusov RL, Sabathe F, Soucaille P, Daly MJ, Bennett GN, Koonin E V, Smith DR (2001) Genome Sequence and Comparative Analysis of the Solvent-Producing Bacterium Clostridium acetobutylicum Genome Sequence and Comparative Analysis of the Solvent-Producing Bacterium Clostridium acetobutylicum. J Bacteriol 183:a823–4838. doi: 10.1128/JB.183.16.4823

Palomo-Briones R, Razo-Flores E, Bernet N, Trably E (2017) Dark-fermentative biohydrogen pathways and microbial networks in continuous stirred tank reactors: Novel insights on their control. Appl Energy 198:77–87. doi: 10.1016/j.apenergy.2017.04.051

Pyne ME, Utturkar S, Brown SD, Moo-Young M, Chung DA, Chou CP (2014) Improved Draft Genome Sequence of Clostridium pasteurianum Strain ATCC 6013 (DSM 525) Using a Hybrid Next-Generation Sequencing Approach. Genome Announc 2:2–3. doi: 10.1128/genomeA.00790-14

R Development Core Team R (2011) R: A Language and Environment for Statistical Computing.

Rochex A, Godon J, Bernet N, Escudier R (2008) Role of shear stress on composition, diversity and dynamics of biofilm bacterial communities. Water Res 42:4915–4922. doi: 10.1016/j.watres.2008.09.015

Saady NMC (2013) Homoacetogenesis during hydrogen production by mixed cultures dark fermentation: Unresolved challenge. Int J Hydrogen Energy 38:13172–13191. doi: 10.1016/j.ijhydene.2013.07.122

Schuchmann K, Müller V (2014) Autotrophy at the thermodynamic limit of life: a

model for energy conservation in acetogenic bacteria. Nat Rev Microbiol 12:809–821. doi: 10.1038/nrmicro3365

Senger RS, Papoutsakis ET (2008) Genome-scale model for Clostridium acetobutylicum: Part I. Metabolic network resolution and analysis. Biotechnol Bioeng 101:1036–1052. doi: 10.1002/bit.22010

Shanmugam SR, Chaganti SR, Lalman JA, Heath DD (2014) Statistical optimization of conditions for minimum H2 consumption in mixed anaerobic cultures: Effect on homoacetogenesis and methanogenesis. Int J Hydrogen Energy 39:15433–15445. doi: 10.1016/j.ijhydene.2014.07.143

Si B, Li J, Li B, Zhu Z, Shen R, Zhang Y, Liu Z (2015) The role of hydraulic retention time on controlling methanogenesis and homoacetogenesis in biohydrogen production using upflow anaerobic sludge blanket (UASB) reactor and packed bed reactor (PBR). Int J Hydrogen Energy 40:11414–11421. doi: 10.1016/j.ijhydene.2015.04.035

Sikora A, Baszczyk M, Jurkowski M, Zielenkiewicz U (2013) Lactic Acid Bacteria in Hydrogen-Producing Consortia: On Purpose or by Coincidence? In: Lactic Acid Bacteria - R & D for Food, Health and Livestock Purposes. InTech,

Sivagurunathan P, Lin C-Y (2016) Enhanced biohydrogen production from beverage wastewater: process performance during various hydraulic retention times and their microbial insights. RSC Adv 6:4160–4169. doi: 10.1039/C5RA18815F

Tracy BP, Jones SW, Fast AG, Indurthi DC, Papoutsakis ET (2012) Clostridia: the importance of their exceptional substrate and metabolite diversity for biofuel and biorefinery applications. Curr Opin Biotechnol 23:364–381. doi: 10.1016/j.copbio.2011.10.008

FIGURE CAPTIONS

Fig. 1 Hydrogen production performance of the CSTR operated under different values of OLR. Box plots of VHPR and H2 yield include all data of the corresponding periods. a) VHPR and OLR b) H2 yield and biomass concentration

Fig. 2 Microbial communities and metabolites productivities of dark fermentative systems under different values of OLR. a) Ward D2 hierarchichal cluster analysis based on Pearson distances; b) CE-SSCP profiles of microbial communities developed under different OLR; c) VFA and hydrogen yields from steady states. B, butyrate; L, lactate; A, acetate; F, formate

Fig. 3 a) Profiles of the microbial communities from the operation of the CSTR at different conditions of OLR obtained by Illumina MiSeq analysis. b) Relationship between Clostridium and Streptococcus species with the OLR

Fig. 4 Principal Components Analysis of biohydrogen production under different OLR.

Table 1

Table 1. Summary of the steady state performance of the dark fermentative CSTR operated under different OLR.

Stage	OLR $g_{lactose}$/L-d	Theoretical[a] VHPR, L_{H2}/L-d	Experimental VHPR, L_{H2}/L-d	H_2 yield mol_{H2}/mol_{Hexose}	H_2 consumed in formate synthesis[b] L_{H2}/L-d	Formate mmol/L	Acetate mmol/L	Lactate mmol/L	Butyrate mmol/L
I	88.2	52.4	13.7 ± 1.3	1.21 ± 0.11	5.72	63.9	26.8	33.4	39.6
II	58.8	34.9	5.5 ± 0.3	0.74 ± 0.04	2.01	22.5	19.3	34.1	23.2
III	44.1	26.2	11.6 ± 0.4	2.08 ± 0.12	0.44	5.0	16.9	3.9	30.1
IV	29.4	17.5	7.8 ± 1.1	2.14 ± 0.45	0.25	2.8	8.6	1.0	13.7
V	22.0	13.1	5.5 ± 0.7	1.93 ± 0.23	0.58	6.5	14.6	3.5	24.7
VI	14.7	8.7	3.2 ± 0.7	1.84 ± 0.73	0.54	6.0	8.0	3.7	7.1
VII	58.8	34.9	14.5 ± 0.1	1.90 ± 0.02	1.47	16.4	10.8	49.7	22.3

[a]Theoretical VHPR based on the theoretical yield of 4 mol_{H2}/mol_{Hexose} and lactose added.

[b]Based on the assumption that formate was produced by the consumption of H_2: $CO_2 + H_2 \rightarrow CHOOH$

Samples considered as steady state = 4, 4, 4, 4, 3, 5, and 3 for stages I-VII, respectively.

Table 2. Growth kinetic parameters of representative species of hydrogen producing bacteria and LAB.

Microorganism	Kinetic conditions	μ_{max}, 1/h	K_S, g/L	Reference
Clostridium acetobutylicum	Lactose, pH 5, 35 °C	0.95	1.34	(Napoli et al. 2011)
Lactococcus casei	Whey-lactose, pH 5.5, 37 °C	0.265	0.72	(Altiok et al. 2006)
Lactobacillus bulgaricus	pH 5.6, 42 °C	1.14	3.36	(Burgos-Rubio et al. 2000)
Lactococcus lactis	Lactose, pH 6.5, 30 °C	1.1	1.32	(Boonmee et al. 2003)
Lactobacillus rhamnosus	Glucose, pH 5.5, 40 °C,	0.45	0.30	(Berry et al. 1999)

Table 3. Gibbs' energy of acetate and formate autotrophic reactions.

	ΔG°	ΔG (Stage VI)	ΔG (Stage I)
$2\ HCO_3^- + 2\ H^+ + 4\ H_2 \rightarrow CH_3COO^- + H^+ + 4\ H_2O$	-144.4 kJ	-101.2 kJ	-98.15 kJ
$HCO_3^- + H^+ + H_2 \rightarrow CHOO^- + H^+ + H_2O$	-1.3 kJ	-35.7 kJ	-29.6 kJ

ΔG° were calculated at 25°C and standard concentrations.

ΔG were calculated at pH 5.9, 37°C and the following concentrations: $[HCO_3^-] = 0.05$ M; $[H_2] = 0.05$M; [VFA] = Table 1.

Gibbs' energy values were computed in accordance with Kleerebezem and Van Loosdrecht (2010).

Figure 1

Click here to download Figure Fig1.jpeg

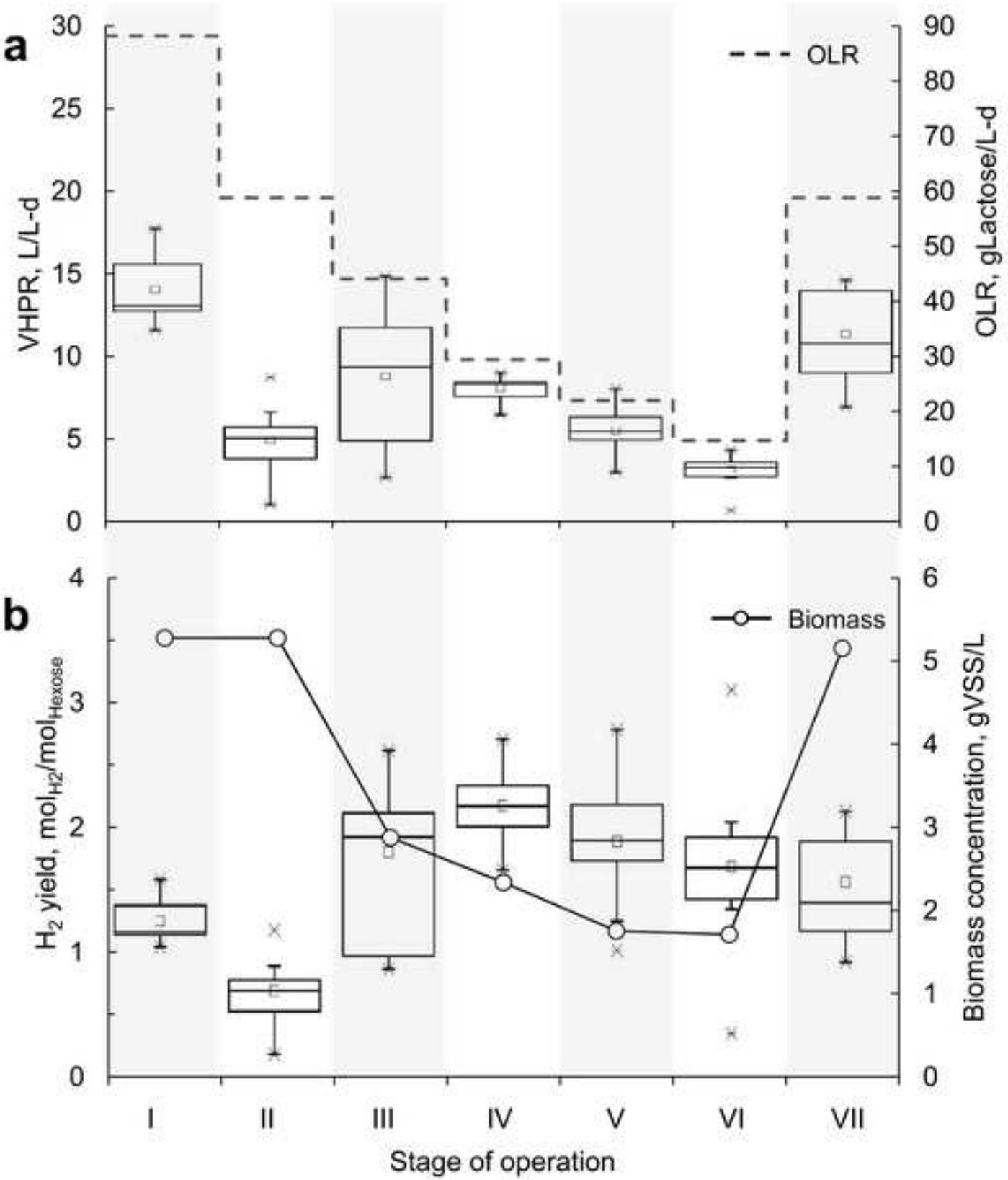

Figure 2

Click here to download Figure Fig2.jpeg

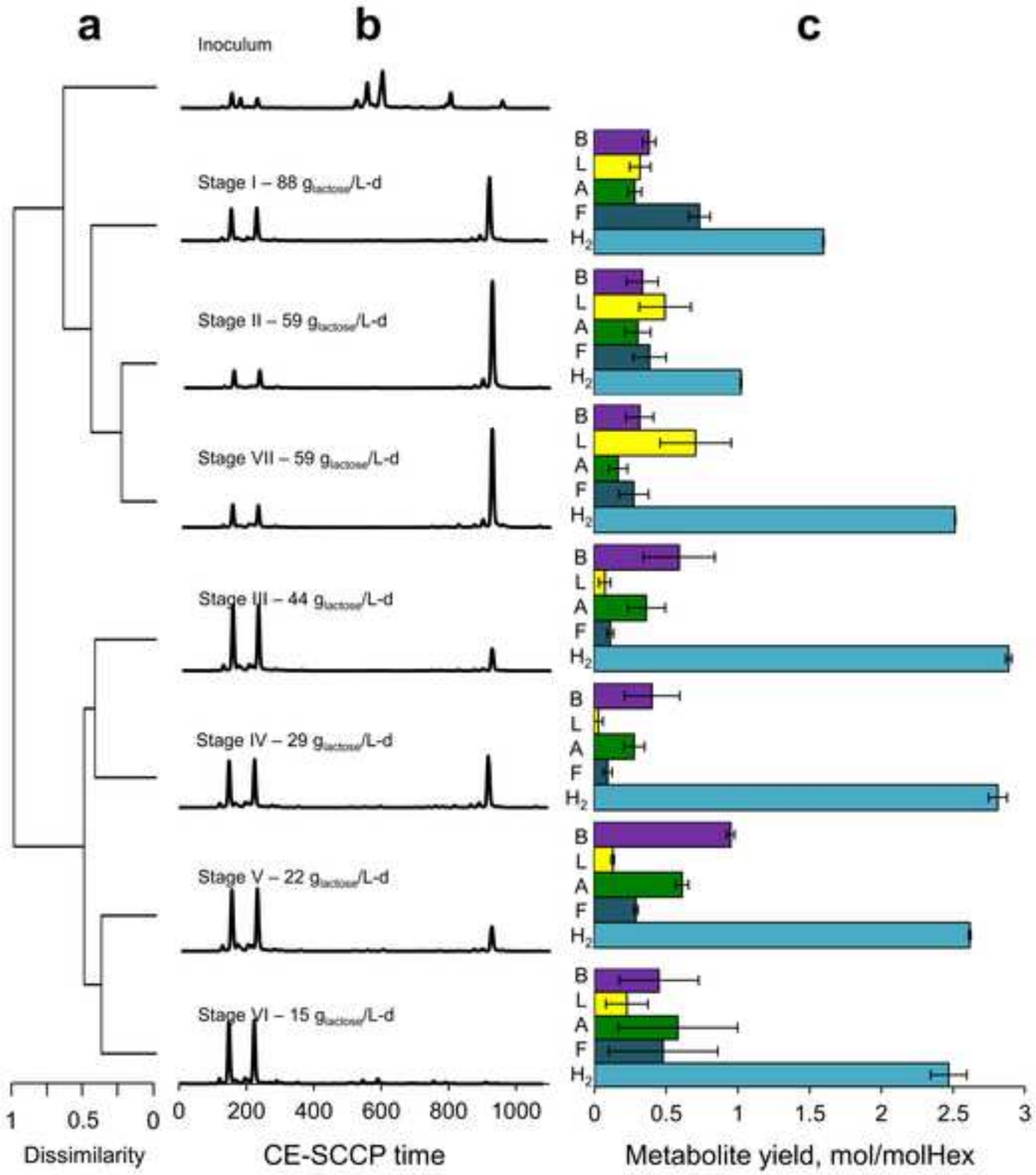

Figure 3

Click here to download Figure Fig3.jpeg

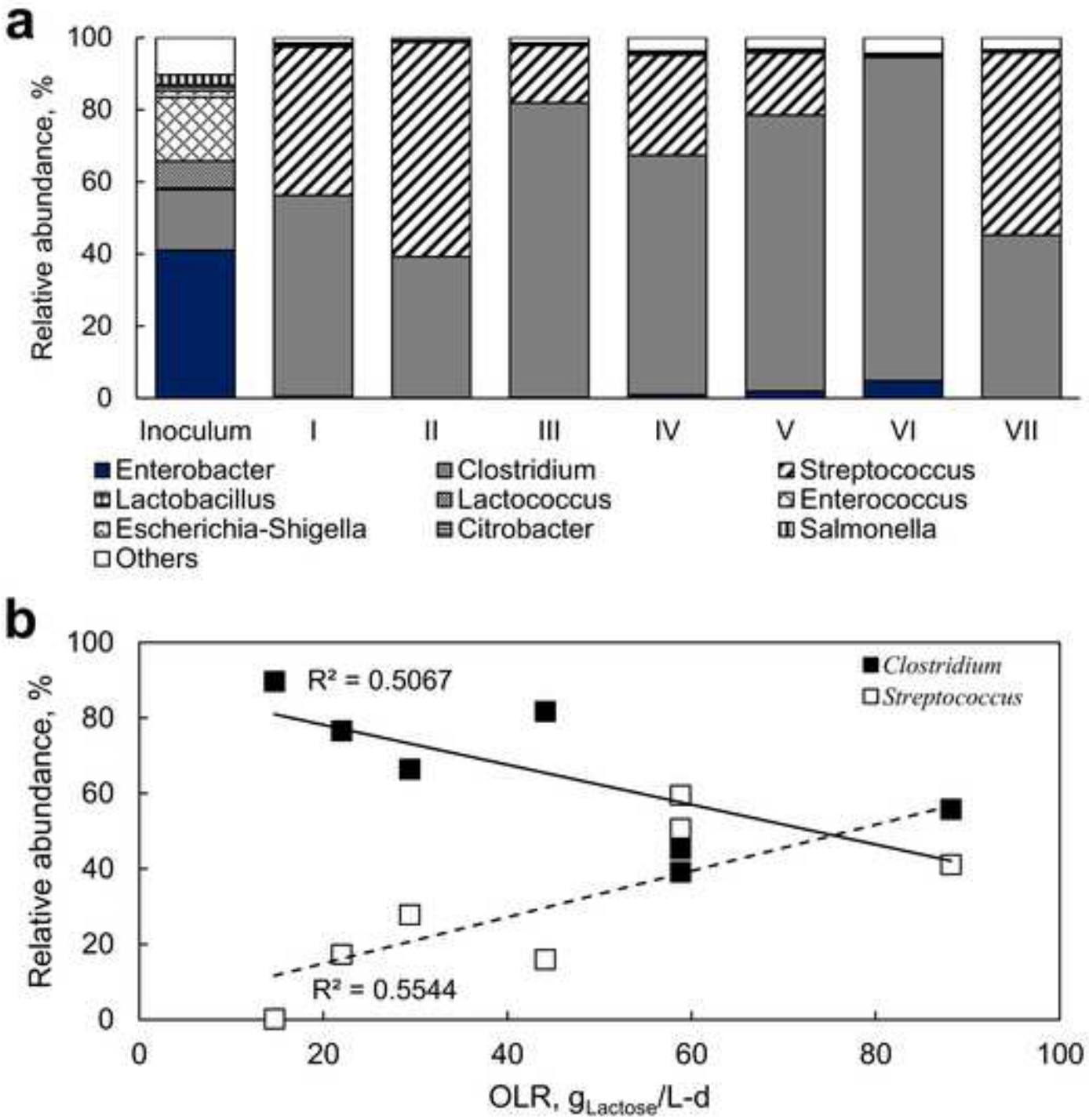

Figure 4

Click here to download Figure Fig4.jpeg